

Boundary-Layer Transition Effects on Airplane Stability and Control

C. P. van Dam*

University of California, Davis, California
and

B. J. Holmes†

NASA Langley Research Center, Hampton, Virginia

Surface contamination of laminar-flow airfoils can significantly modify the location of transition from laminar-to-turbulent boundary-layer flow. The contamination can be the result of insect debris, environmental effects such as ice crystals and moisture due to mist or rain, surface damage, or other contamination adhering to the surface. Location and mode of transition have a dominant effect on the lift-and-drag characteristics of a lifting surface. The influences of laminar boundary-layer flow behavior on airplane stability and control are examined through theoretical results and experimental (wind tunnel and free-flight) data. For certain airfoils with a relatively steep pressure recovery, it is shown that loss of laminar flow near the leading edge can result in premature separation of the turbulent boundary layer and, consequently, in loss of lift and control effectiveness. Aerodynamic modifications that minimize boundary-layer transition effects on airplane stability and control are also discussed.

Nomenclature

A	= aspect ratio, b^2/S
b	= wing span, ft
C_L	= airplane lift coefficient
$C_{L\alpha}$	= lift-curve slope, rad^{-1}
C_m	= airplane pitching-moment coefficient
$C_{m\alpha}$	= variation of pitching-moment coefficient with angle of attack, rad^{-1}
C_n	= airplane yawing-moment coefficient
$C_{n\beta}$	= variation of yawing-moment coefficient with angle of sideslip, rad^{-1}
c	= chord length, ft
\bar{c}	= mean aerodynamic chord, ft
c_d	= section drag coefficient
c_l	= section lift coefficient
$c_{l\alpha}$	= section lift-curve slope, rad^{-1}
c_m	= section pitching-moment coefficient
N	= airplane yawing moment, ft-lb
q	= dynamic pressure, lb/ft^2
R	= chord Reynolds number
S	= lifting-surface reference area, ft^2
t	= airfoil maximum thickness
U_∞	= freestream velocity, ft/s
V_i	= indicated airspeed, knots or mph
v	= local velocity, ft/s
\bar{x}	= nondimensional longitudinal location, X/\bar{c}
x	= airfoil abscissa, ft
α	= angle of attack, deg
β	= angle of sideslip, deg
δ_e	= elevator deflection, deg
ζ	= damping ratio

ρ	= air density, lb/ft^3
ω_n	= undamped natural frequency, rad/s

Subscripts

ac	= aerodynamic center
C	= foreplane
$c.g.$	= center of gravity
P	= phugoid mode
SP	= short-period mode
t	= transition location
WB	= wing body
WLT	= winglet

Introduction

IN recent years, airplane construction materials and fabrication methods have improved greatly, resulting in the production of airframe surfaces with very little roughness and waviness, which accurately match the design shape. Flight tests^{1,2} have demonstrated that extensive runs of laminar boundary layer flow can be obtained over regions of favorable pressure gradient on modern airplane surfaces and that these can provide a significant reduction in the level of skin friction and in the value of profile drag. Loss of laminar flow can be caused by surface contamination such as insect debris,³ ice crystals,⁴ moisture due to mist or rain,⁵ and surface damage.⁶ Also, "innocent" minor modifications, such as the addition of a spanwise paint stripe, can trip the boundary layer and result in premature transition from laminar-to-turbulent flow.⁷ Consequently, the application of natural laminar flow (NLF) to modern aircraft designs has raised new issues concerning airplane performance and stability-and-control characteristics. These issues relate to the certification of aircraft with extensive regions of laminar flow. Specifically, to varying degrees depending on individual NLF airfoil behavior, loss of laminar flow may result in significantly diminished airplane performance and substantial changes in airplane stability and control. Therefore, special Federal Aviation Administration Airworthiness Regulations may be necessary as part of the certification process of future aircraft designs that incorporate laminar boundary-layer flow. (The Appendix presents proposed wording for the special conditions for certification of the

Presented as Paper 86-2229 at the AIAA Atmospheric Flight Mechanics Conference, Williamsburg, VA, Aug. 18–20, 1986; received Feb. 19, 1987; revision received June 29, 1987. This paper is declared a work of the U.S. Government and is not subject to copyright protection in the United States.

*Assistant Professor, Department of Mechanical Engineering, Division of Aeronautical Science and Engineering. Member AIAA.

†Head, Flight Applications Branch, Low Speed Aerodynamics Division. Senior Member AIAA.

Beechcraft Model 2000 airplanes. These special conditions address the procedures for certification of the performance and handling qualities of the airplane that may be affected by laminar boundary-layer behavior.)

The purpose of this paper is to examine the effects of laminar-flow behavior on airplane stability and control. The first part of the paper presents the physics of the potential adverse effects of premature boundary-layer transition on airfoil characteristics. A combination of theoretical and experimental results will be used to illustrate the various phenomena. In the second part of the paper, the potential effects of laminar-flow behavior on total airplane stability and control are examined. Examples are provided illustrating the changes in stability-and-control characteristics for various airplanes.

Laminar Boundary-Layer Behavior and Airfoil Aerodynamic Characteristics

The boundary-layer phenomena that provide the mechanisms by which airplane stability and control can be influenced by laminar behavior include changes in transition location and mode of transition, and the ensuing changes in turbulent separation location. For a two-dimensional section, transition can result from viscous Tollmien-Schlichting (T-S) instability, or from inflectional instability at laminar separation. For three-dimensional flows, such as can be encountered on swept wings, two additional transition modes of practical interest are the crossflow (inflectional) instability and turbulent contamination of the attachment-line flow.

Recent flight transition experiments⁵ have demonstrated that in the moderate Reynolds-number flight environment transition often occurs in the separated shear layer of a closed laminar bubble. Transition can also take place in the attached boundary layer, resulting from growth of two-dimensional (T-S) disturbances in the laminar boundary layer. This two-dimensional disturbance growth is accelerated by surface roughness and waviness. The initial conditions for the turbulent boundary layer that originate in the free-shear layer at laminar separation are quite different, compared to the initial conditions of a turbulent boundary layer that originates in the attached boundary layer. The downstream behavior of the turbulent boundary layer can be dramatically affected by the mode of transition.

The location of transition can influence the ensuing location of turbulent separation, thus affecting both the aerodynamic characteristics of an airfoil and the effectiveness of trailing-edge control surfaces. The initiator of transition that is perhaps most important to the present discussion of airplane stability and control is environmental surface contamination caused by insects, ice, rain, or crystalline cloud particles. The surface roughness caused by such contamination can lead to early transition near the leading edge. A turbulent boundary layer that originates near the leading edge of an airfoil, substantially ahead of the point of minimum pressure, will produce a thicker boundary layer at the onset of pressure recovery, as compared to the conditions produced by a turbulent boundary layer that originates further downstream. With sufficiently steep pressure gradients in the recovery region, a change in turbulent boundary layer conditions resulting from changes in transition location or mode of transition can lead to premature turbulent separation. This behavior will be demonstrated by presenting the results of analytical and experimental examinations of the aerodynamic characteristics for several airfoil sections.

In Fig. 1, the geometry and two inviscid velocity distributions are shown for the GU25-5(11)8 airfoil section.⁸⁻¹⁰ The section characteristics have been calculated using the incompressible airfoil design and analysis method developed by Eppler and Somers.¹¹ This airfoil section has a $t/c = 0.20$, and maximum thickness is located at $x/c = 0.416$. The GU25-5(11)8 is capable of generating high maximum lift coefficient at relatively low Reynolds numbers and, consequently, a large number of foreplane designs for homebuilt configurations use this section shape. The velocity distributions in Fig. 1 indicate

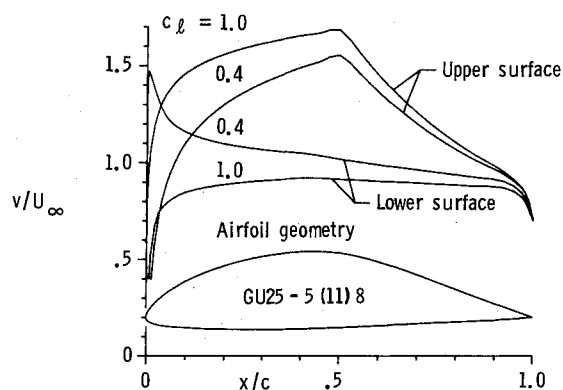


Fig. 1 Geometry and inviscid velocity distributions of GU25-5(11)8.

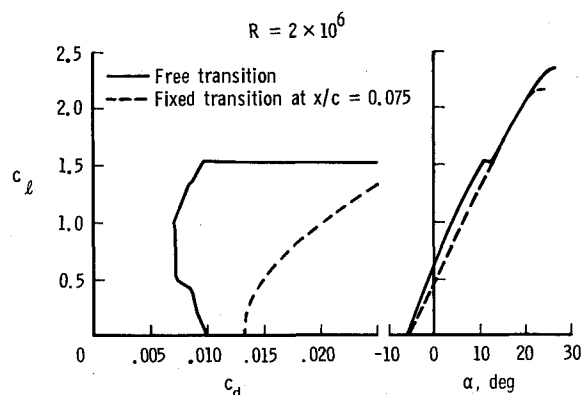


Fig. 2 Calculated aerodynamic characteristics of GU25-5(11)8 at $R = 2 \times 10^6$.

that at $x/c \approx 0.50$ the favorable accelerating flow condition over the front portion of the airfoil abruptly changes to an adverse decelerating flow condition over the aft portion of the airfoil. This type of flow discontinuity causes the laminar boundary layer to separate. Transition will occur in the free-shear layer and the boundary layer will reattach in the turbulent state. The method of Ref. 11 models the location of laminar separation, but not the bubble nor its influence on the pressure distribution and airfoil lift-and-drag characteristics. The method predicts the influence of turbulent separation on airfoil aerodynamic characteristics through a simple scheme. In Fig. 2, calculated lift-and-drag results are presented for a typical chord Reynolds number $R = 2 \times 10^6$, and the results clearly illustrate the influences of loss of laminar flow. The free-transition results show that airfoil aerodynamic characteristics change dramatically at $\alpha \approx 10$ deg. At that angle of attack, a sharp upper-surface leading-edge suction peak causes transition to move forward suddenly. With this forward shift of transition, turbulent separation at the trailing edge increases and a loss in lift is encountered. Also, forward movement of transition location and turbulent separation produce a large increase in section drag. The lift-and-drag characteristics of the airfoil section change drastically when transition location is fixed near the leading edge, simulating the condition when the leading edge of the airfoil section is critically contaminated by insects or moisture. The section drag increases significantly, as expected. However, the results of Fig. 2 indicate that both section lift-curve slope $c_{l\alpha}$, and section maximum lift coefficient $c_{l\max}$ are reduced with fixed leading-edge transition. For the GU25-5(11)8 airfoil section, these calculations illustrate the significant effects of boundary-layer transition near the leading edge and the ensuing premature separation of the turbulent boundary layer.

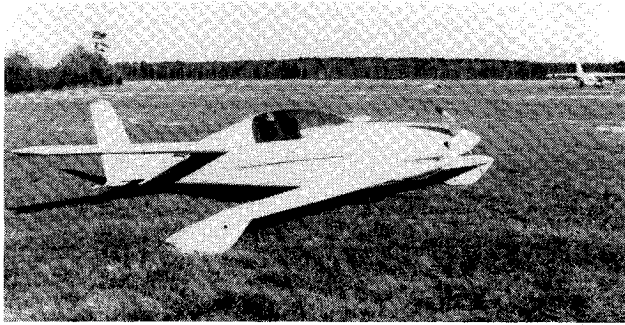


Fig. 3 Dragonfly tandem-wing airplane utilized in NLF flight experiment.

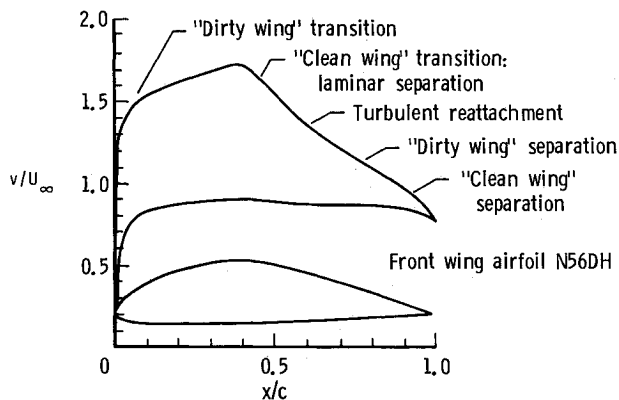


Fig. 4 Inviscid velocity distribution and calculated transition and separation locations for Dragonfly foreplane section shape ($\alpha = 4$ deg, $R = 2 \times 10^6$).

Laminar-flow flight experiments were conducted on the Dragonfly airplane illustrated in Fig. 3. The airplane is a two-place, single-engine, tractor, tandem-wing configuration that incorporates an airfoil section similar to the GU25-5(11)8. In Fig. 4, the "as-built" section shape of the foreplane airfoil on the Dragonfly is shown. [The Dragonfly (N56DH) used in these experiments incorporates a foreplane airfoil section modified from the original plans, with slightly increased thickness and slightly further forward maximum thickness location]. Also, in Fig. 4, the surface velocity distribution is depicted for a typical climb or approach speed of 80 mph. The locations of boundary-layer transition and turbulent separation are indicated for free and fixed ($x/c = 0.075$) transition. In the case of free transition, laminar separation is predicted near $x/c = 0.50$. Separation of the turbulent boundary layer then is predicted near $x/c = 0.95$. For the airfoil with transition fixed near the leading edge, the resulting turbulent boundary layer is unable to remain attached during the pressure recovery on the aft part of the airfoil, and it separates near $x/c = 0.75$, much further forward than for the free transition case.

The aspect ratio of the foreplane is moderate ($A = 8.3$) and, consequently, good agreement can be expected between the predicted two-dimensional characteristics and the behavior of the three-dimensional surface. Several flow-visualization flight tests were conducted using a thin coating of SAE 10W-40 motor oil darkened with lampblack, and brushed on the smooth wing surface. For airplane speeds in the range of 70 to 110 mph, a laminar separation bubble was found on the front wing beginning at $x/c = 0.45$, with turbulent reattachment at $x/c = 0.55$, as evident by pooling of the oil in the region as it flowed in a forward direction. The turbulent-flow region aft of the bubble was clearly marked by an uneven, stringy flow of the oil towards the aft portion of the wing, where the oil once again pooled as the turbulent flow separated from the wing. At

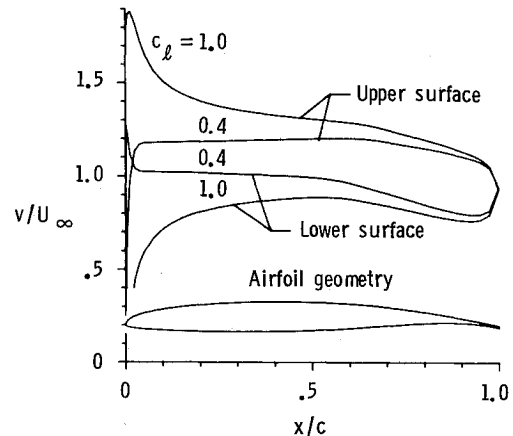


Fig. 5 Aerodynamic characteristics for a typical winglet airfoil.

80 mph, turbulent separation occurred just ahead of the elevator at $x/c = 0.70$. Thus, the predicted boundary-layer behavior previously discussed roughly agrees with the free-transition behavior observed in flight. The difference between the location of predicted turbulent separation ($x/c = 0.95$) and the measured location ($x/c = 0.70$) may be accounted for by two factors. First, the prediction does not account for the effect of the length of the laminar separation bubble (about 10% chord in length) to promote earlier turbulent separation. Second, the prediction does not account for the potentially deteriorating effect of flow through the elevator slot. No flow-visualization tests were conducted with fixed transition on the foreplane leading edge because of the inadequate climb performance observed in this condition. It was believed that this large performance degradation was caused by massive turbulent separation.

The two airfoils that have been analyzed previously both display relatively thick section shape, which contributes to the significant influence of laminar behavior on their aerodynamic characteristics. For thin airfoils with relatively sharp leading edge, laminar stall, which is caused by bursting of the laminar separation bubble, may seriously affect section lift-and-drag characteristics and, thus, airplane stability and control. Next, the influence of laminar boundary-layer behavior on the aerodynamic characteristics of a relatively thin airfoil section is analyzed.

Initial airfoil sections recommended for winglet applications on high-speed subsonic aircraft were developed to operate at high Mach number design conditions and were cambered to obtain satisfactory high-lift characteristics.¹² In order to avoid creating shock waves on the upper winglet surface and to minimize the added induced velocities on the wing tip upper surface associated with the winglet, the thickness ratio was held to 8%. Subsequent winglet designs for low-speed airplanes have also used this airfoil section in a number of cases. However, this airfoil section was not specifically designed for low Reynolds number or low-speed applications. The airfoil performance under these conditions can be improved.¹³

In Fig. 5, airfoil section shape and two inviscid velocity distributions for the original supercritical airfoil are shown. At a typical cruise $c_l = 0.4$, the velocity gradient on the upper surface is favorable up to $x/c = 0.65$. Flight tests have shown that transition on the smooth upper surface of a winglet utilizing this section shape occurs at $x/c \approx 0.70$ at low lift coefficient (Fig. 6). On the lower surface, however, a sharp suction peak occurs near the leading edge. With decreasing angle of attack, this suction peak over the highly curved leading edge grows rapidly, and the integral boundary-layer method of Ref. 11 predicts leading-edge flow separation on the lower surface for angles of attack less than about -5 deg (Fig. 7). The loss in lift

and the increase in drag associated with boundary-layer separation can have a detrimental influence on airplane directional stability and control. As shown in Fig. 7, the thin airfoil section achieves a high maximum lift coefficient, but the laminar bucket is relatively narrow and starts and ends very abruptly. With the shallow pressure recovery, however, turbulent separation and section lift characteristics are not affected by loss of laminar flow. Leading-edge separation caused by bursting of the laminar bubble can produce loss in lift and large increases in drag for thin airfoil sections. Moreover, thin laminar-flow sections tend to display narrow and sharply defined laminar buckets.

Airplane Longitudinal Stability and Control

In the previous section, the influence of location and mode of transition from laminar to turbulent boundary-layer flow on airfoil aerodynamic characteristics has been discussed. It has been shown that for certain airfoils extensive trailing-edge separation of the turbulent boundary layer can occur if the boundary layer becomes turbulent near the leading edge. This boundary-layer separation results in a loss of lift, and the resulting effects on airplane longitudinal stability and control characteristics are discussed next.

Wind tunnel experiments have been conducted with a canard configuration that uses a high-aspect-ratio foreplane with the GU25-5(11)8 section shape. Holmes et al.² and Yip and Coy¹⁴ presented full-scale, model-wind tunnel data depicting the influence of transition location on longitudinal characteristics for

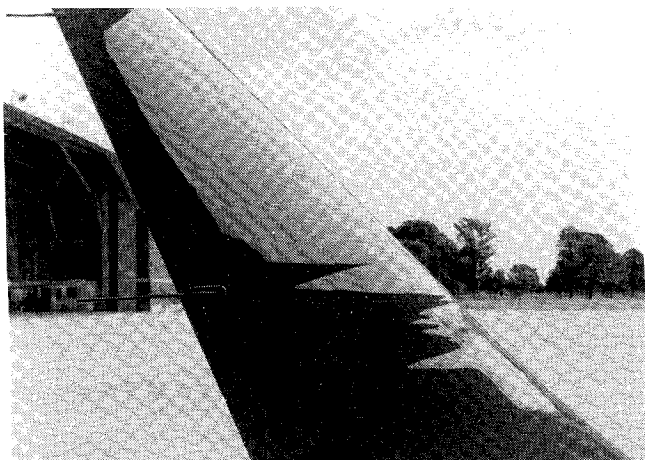


Fig. 6 Transition on Learjet winglet indicated by sublimating chemicals ($M = 0.62$, $R = 2.5 \times 10^6 \text{ ft}^{-1}$).

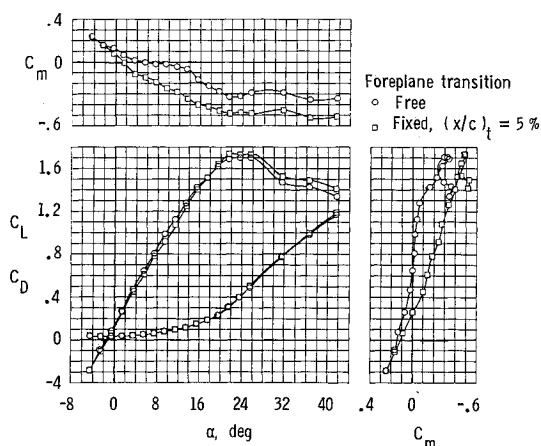


Fig. 7 Calculated aerodynamic characteristics of winglet airfoil section.

a VariEze airplane. In the previous section it has been demonstrated that transition location has a dramatic influence on the lift characteristics of the GU25-5(11)8 airfoil section. Notably, a reduced section lift-curve slope caused by fixed boundary-layer transition near the leading edge was observed. In subsonic-flow conditions, foreplane lift-curve slope $C_{L_{\alpha,C}}$ is a function of $c_{l_{\alpha}}$, Mach number and several planform parameters and, thus, a reduction in $c_{l_{\alpha}}$ results in a reduced value for $C_{L_{\alpha,C}}$. In Fig. 8, airplane pitching-moment coefficient results clearly demonstrate the large influence of foreplane transition location on airplane longitudinal aerodynamic characteristics. Airplane longitudinal static stability for a canard configuration can be written as follows:

$$C_{m_{\alpha}} = C_{L_{\alpha,C}}(\bar{x}_{c,g} - \bar{x}_{ac,C}) \frac{S_C}{S} + C_{L_{\alpha,WB}}(\bar{x}_{c,g} - \bar{x}_{ac,WB}) \quad (1)$$

where

$$\bar{x}_{ac,WB} > \bar{x}_{c,g} > \bar{x}_{ac,C}$$

A reduction in $C_{L_{\alpha,C}}$, as a result of foreplane flow separation, makes the first term on the right-hand side of Eq. (1) less positive, which results in an increased nose-down pitching moment. Eq. (1) can also be written as

$$C_{m_{\alpha}} = C_{L_{\alpha}}(\bar{x}_{c,g} - \bar{x}_{ac}) \quad (2)$$

where $C_{L_{\alpha}}$ represents the lift-curve slope of the complete airplane and \bar{x}_{ac} indicates the longitudinal location of the airplane aerodynamic center. The data of Fig. 8 are for a constant foreplane control surface deflection ($\delta_e = 0$ deg), and as a result $(\bar{x}_{c,g} - \bar{x}_{ac})$ can be defined as airplane stick-fixed static margin. For these wind tunnel test conditions, the influence of fixed leading-edge transition on $C_{L_{\alpha}}$ is relatively small, as shown in Fig. 8. In the angle-of-attack range from 3 to 13 deg, the tunnel data show that airplane static margin is about $0.10 \bar{c}$ in the case of free transition on the foreplane. When transition is fixed near the foreplane leading edge, the airplane becomes longitudinally much more stable and the static margin is about $0.30 \bar{c}$. Thus, airplane aerodynamic center shifts rearward over a distance of $0.20 \bar{c} \approx 6$ in. as a result of foreplane trailing-edge flow separation.

The VariEze airplane configuration tested in the full-scale wind tunnel has also been tested in flight with and without artificial roughness near the leading edge of the foreplane. The changes in foreplane lift characteristics with fixed transition affect elevator-deflection required to trim the airplane for a given airspeed, as shown in Fig. 9. Fixed leading-edge transition induces flow separation on the foreplane and, thus, increased positive elevator deflection is required to obtain a foreplane lift coefficient that provides longitudinal trim. The effect of fixed transition on airplane lift characteristics is de-

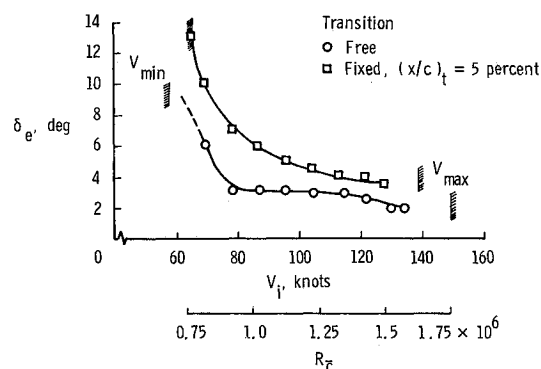


Fig. 8 Longitudinal aerodynamic characteristics of a canard configuration as tested in NASA Langley 30 x 60 ft wind tunnel.

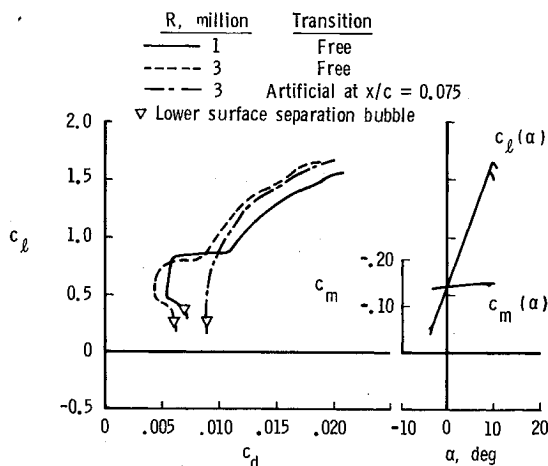


Fig. 9 Flight measured longitudinal control characteristics for VariEze canard-configured airplane ($\bar{c} = 1.08$ ft).

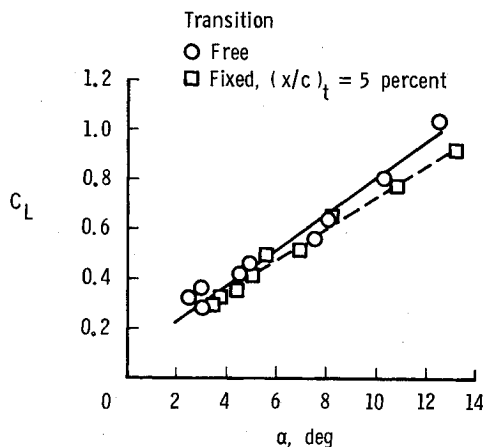


Fig. 10 Flight measured lift characteristics for VariEze canard-configured airplane.

picted in Fig. 10. These flight-test data demonstrate that the lift-curve slope is reduced by 7%, while the wind tunnel results (see Fig. 8) indicate a reduction in airplane $C_{L\alpha}$ of less than 4%.

The source of this discrepancy is that the wind tunnel data have been obtained untrimmed for a constant elevator deflector $\delta_e = 0$ deg, whereas the flight data have been obtained for elevator deflection required to trim the airplane. In level flight, lower airspeed results in higher airplane lift coefficient and, therefore, more positive elevator deflection is required for airplane trim, as shown in Fig. 9. Trailing-edge flow separation increases with increasing elevator deflection, producing further lift loss. A second contributing factor is the influence of Reynolds number on lift. Level-flight data at high-lift coefficients are obtained at relatively low Reynolds numbers, as compared to the Reynolds numbers encountered at low lift coefficients. The following expression depicts this effect more clearly:

$$\frac{R_1}{R_2} = \sqrt{\frac{C_{L2}}{C_{L1}}} \quad (3)$$

where it has been assumed that airplane weight and flight altitude are constant. The reduced Reynolds number at higher lift coefficients increases foreplane flow separation.

In the previous section, the foreplane section characteristics for a Dragonfly airplane (Fig. 3) have been analyzed. In the case of a clean surface, it has been shown that a large separation bubble exists at the onset of pressure recovery for climb-

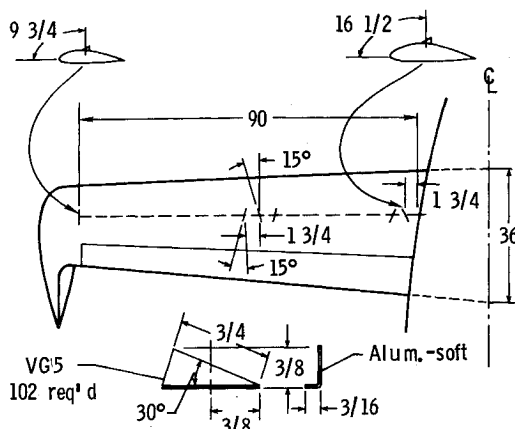


Fig. 11 Sketch of vortex generator installation (dimensions in inches).

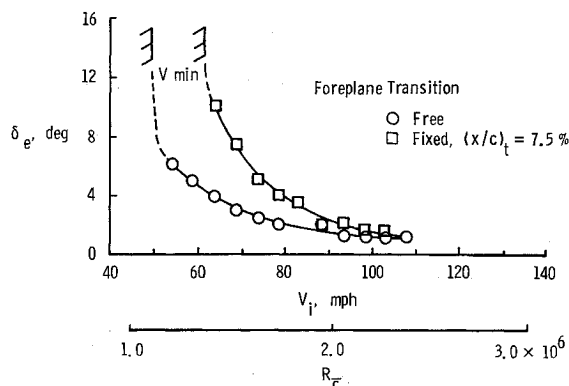


Fig. 12 Influence of transition location on pitch control characteristics of tandem-wing configuration (vortex generators installed on foreplane, $\bar{c} = 2.36$ ft).

and-approach angle of attack. The laminar bubble causes poor climb performance after takeoff and undesirable landing characteristics due to high airplane stall speed. In order to minimize the adverse effects of laminar separation and leading-edge surface contamination on the aerodynamic characteristics of the foreplane, vortex generators were fastened to the surface just ahead of the bubble front edge. Wentz¹⁵ and Bragg and Gregorek⁷ present detailed information on the influence of vortex generators on section characteristics of several airfoils. The vortex generators are very small, low-aspect-ratio wings positioned at a high angle of incidence with respect to the local flow direction. The purpose of the vortex generators used on the Dragonfly is twofold: 1) A vortex generator in a laminar boundary layer acts as a three-dimensional disturbance that causes boundary-layer transition and prevents laminar separation, thus changing the mode of transition, and 2) The device produces a vortex which energizes the turbulent boundary layer and reduces turbulent separation.

In Fig. 11, the location and geometry of the foreplane vortex generators are sketched. The vortex generators dramatically change the minimum and maximum airspeed of the airplane. The minimum airspeed drops from an indicated airspeed of 59 to 50 mph, while the maximum indicated airspeed increases from 140 to 150 mph. Airplane pitch-control data indicate that less downward deflection of the elevators is required with vortex generators on the upper surface, improving foreplane lift characteristics. In Fig. 12, the effect of leading-edge contamination on airplane pitch control is shown for the foreplane with vortex generators installed. More elevator deflection is required to trim the airplane at a given airspeed with transition fixed near the leading edge, indicating that vortex generators in

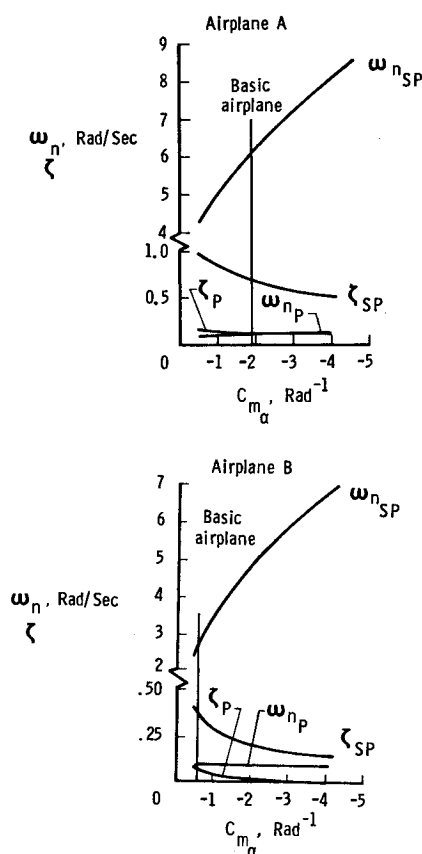


Fig. 13 Effect of airplane pitching-moment-coefficient curve slope on longitudinal dynamic stability characteristics: a) airplane A at 5000 ft and $M = 0.31$; b) airplane B at 40,000 ft and $M = 0.7$.

this location only partly correct the loss in lift resulting from leading-edge transition. It should be noted, however, that the airplane without vortex generators, yet with surface contamination on the foreplane, has severely degraded handling qualities at low airspeeds. The airplane in this configuration has an estimated minimum airspeed of 80 mph, but no additional test data were obtained because of the degraded handling qualities. The results obtained with the tandem-wing configuration demonstrate that vortex generators located just ahead of laminar separation onset are very effective in eliminating the laminar separation bubble and its adverse effects for a smooth foreplane surface. However, the adverse influence on foreplane lift characteristics of a forward shift in transition location with surface contamination is only partly corrected by the vortex generators. These in-flight observed effects of vortex generators are in good agreement with the wind tunnel results of Bragg and Gregorek.⁷

The large change in variation of pitching-moment coefficient with angle of attack $C_{m\alpha}$, resulting from premature foreplane separation, also has a strong effect on airplane longitudinal transient behavior. The influence of $C_{m\alpha}$ on the undamped natural frequency of the short period can be estimated as follows:

$$\frac{\omega_{nSP,1}}{\omega_{nSP,2}} = \sqrt{\frac{C_{m\alpha,1}}{C_{m\alpha,2}}} \quad (4)$$

Thus, an increase in the value of $C_{m\alpha}$ by a factor 3, as observed in Fig. 8, causes ω_{nSP} to increase by more than 70%. Although a complete set of stability derivatives was not available for a canard type of airplane, Fig. 13 shows a derivative sensitivity analysis for two conventional airplanes for which stability derivatives are presented in Ref. 16. Airplane A (Fig. 13a) is representative of a twin-engine propeller-driven airplane; air-

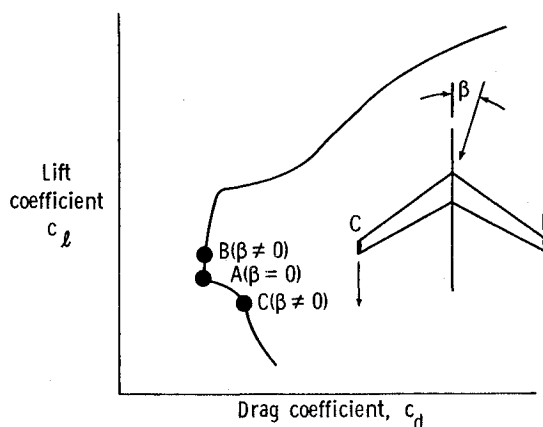


Fig. 14 Drag polar of winglet airfoil with "sharply defined" drag bucket.

plane B (Fig. 13b) is representative of a twin-engine business jet. The results of Fig. 13 illustrate the magnitude of the influence of $C_{m\alpha}$ on ω_{nSP} . Also, short-period damping ζ_{SP} decreases due to enhanced longitudinal stability.

The results in Fig. 13 demonstrate that phugoid damping ζ_P reduces due to increased longitudinal static stability. This observation matches flight results in a Long-EZ, canard-configuration airplane with a GU25-5(11)8 foreplane section shape. The airplane geometry and transition behavior are described in Ref. 2. When evaluating airplane handling qualities with fixed foreplane transition, a significant reduction in phugoid damping and indications of a slight reduction in short period damping were observed, as compared to damping with free transition on the foreplane. These reductions in damping may be explained as a consequence of the flight-measured reduction in lift curve slope caused by fixed transition.

Airplane Directional Stability and Control

A recent development in the area of airplane design is the utilization of wing tip-mounted winglets to provide directional stability and control in addition to lift-induced drag reduction. The design of winglet airfoil sections, however, has not received much attention, and some winglet designs for low-speed airplanes have adopted the airfoil section shown in Fig. 5. As mentioned previously, this section shape was developed for winglet application at supercritical, high Mach number conditions. Further, this airfoil was designed with the assumption that the flow over the nature airfoil would be turbulent, primarily as a result of surface imperfections. Subsequent flight test results indicated, however, that a winglet with such a section shape can achieve significant regions of laminar flow,^{2,17} as shown in Fig. 6.

There are two mechanisms by which directional stability can be affected by laminar boundary-layer flow behavior. One mechanism involves separation, and the other involves drag asymmetry. In order to prevent changes in airplane directional stability, it is important that the lift characteristics of laminar surfaces that provide directional stability are not affected by premature boundary-layer transition near the leading edge. As previously discussed, premature transition near the leading edge can induce premature turbulent separation in the pressure recovery region of certain thicker laminar-flow airfoils, thus reducing section lift-curve slope and maximum lift. A reduction in the lift-curve slope of such a lifting surface resulting from leading-edge roughness can reduce directional stability significantly. On many existing airplanes, turbulent sections such as the symmetrical NACA four digit series are selected for vertical stabilizers. The lift characteristics of these airfoil sections are not significantly affected by typical surface roughness. For most laminar-flow airfoil sections, including most of the NACA 6-series, premature transition resulting from practical roughness does not influence lift characteristics.

A "sharply defined" airfoil section drag bucket is a concern when the winglets also provide directional stability. Figure 14 also shows the drag polar of the winglet airfoil section, and it illustrates the mechanism by which laminar behavior can produce asymmetric drag forces affecting directional stability. Point A in Fig. 14 represents the cruise condition at a sideslip angle $\beta = 0$ deg. A small positive excursion in sideslip angle causes an increase in angle of attack and, as a result, increased c_d (point B) for the upward winglet and decreased angle of attack and c_d (point C) for the downwind winglet. Section drag at the lower corner of the drag bucket changes rapidly and abruptly. A significant profile drag differential between the two winglets results from the rapid chordwise movement of boundary-layer transition on the lower surface of the airfoil. This force differential produces a destabilizing yawing moment and can create undesirable airplane handling quantities. The change in the yawing moment coefficient produced by the profile-drag differential is ($\beta > 0$)

$$\Delta C_n = -\frac{\Delta C_D}{4} \cdot \frac{S_{WLT}}{S/2} \quad (5)$$

For conventional airplane configurations, the ratio $S_{WLT}/(S/2)$ has a value of 0.02–0.10, and as a result the effect of this destabilizing yawing moment is small. Some canard or flying-wing configurations, however, use winglets to provide directional stability and control, and because of the relatively short moment arm, the winglet area must be large to provide sufficient directional stability. In that case $S_{WLT}/(S/2)$ can be greater than 0.20. An area ratio of that value combined with a ΔC_D of 50 drag counts generates a destabilizing yawing moment ($\beta > 0$) $\Delta C_n = -0.00025$, with a sideslip excursion of less than 0.5 deg. Thus, the destabilizing contribution to the airplane directional stability derivative for small sideslip angles may be of the order of $\Delta C_{n\beta} \approx -0.03 \text{ rad}^{-1}$. This value is large enough to produce nonlinearities in the rudder force and rudder deflection variation with sideslip angle. Such an effect of laminar-flow behavior can significantly influence automatic flight control gain optimization as well as basic airplane stability and control.

Conclusion

Theoretical and experimental results presented in this paper demonstrate that airfoil behavior associated with transition from laminar-to-turbulent boundary-layer flow can significantly affect airplane stability and control. For certain airfoils with a relatively steep pressure recovery, it has been shown that loss of laminar flow near the leading edge can result in trailing-edge separation of the turbulent boundary layer. The aerodynamic parameters that can be adversely affected by the changes in boundary-layer state include maximum lift coefficient, lift-curve slope, and control-surface effectiveness.

Current laminar-airfoil design practice dictates that section shapes for laminar lifting surfaces be utilized that are not susceptible to significantly increased turbulent separation with fully turbulent flow. The analyses presented in this paper reinforce this design practice. An additional requirement for vertical lifting surfaces such as winglets, which provide directional stability, is that section drag should change gradually with angle of attack. If the airfoil drag characteristics display a "deep" and "sharply defined" laminar bucket, then significant nonlinear changes in drag with angle of attack will occur. These undesirable effects can be avoided by design.

The analyses presented in this paper demonstrate that careful design of laminar surfaces is required to minimize adverse effects as a result of changes in laminar boundary-layer transition location or mode of transition. Therefore, it is recommended that fixed transition (near the leading edge) analysis and tests be included as a standard procedure in research and certification evaluations for airplanes with surface smoothness and pressure gradients designed to support laminar flow. This procedure would verify that the airplane with contaminated

surfaces still complies with the Federal Airworthiness Regulations and would document the changes in airplane performance resulting from the loss of laminar flow.

Appendix

The following statements are taken from a notice¹⁸ in which special certification conditions are proposed for the Beech Model 2000 series airplanes. The conditions presented in this appendix address the certification procedure of airplane performance and handling qualities that may be affected by laminar boundary-layer behavior:

"... The airplane will have novel and unusual design features when compared to the state of technology envisaged in the airworthiness standards of 14 CFR Part 23 of the Federal Aviation Regulations (FAR).

These novel and unusual design features include the use of advanced composite materials for primary flight structure, an electronic flight instrument system, the location of the propellers, the aerodynamic configuration, and an outward opening, main entry door in the pressurized cabin, for which the regulations do not contain adequate or appropriate airworthiness standards. This notice contains the additional safety standards that the Administrator considers necessary to establish a level of safety equivalent to that provided by the airworthiness standards of Part 23....

Beech has selected airfoil designs for the Beech Model 2000, having airfoil pressure gradient characteristics and smooth aerodynamic surfaces that may be capable of supporting natural laminar flow. Changes in flying qualities and performances may occur due to the loss of natural laminar flow caused by rain, insects, ice, or other contamination adhering to aerodynamic surfaces.

Airfoil sections, whose performance and flying qualities are substantially degraded by contamination, which would normally be encountered in service, were not envisaged by the existing Part 23 requirements. A special condition is proposed to require that the airplane comply with the requirements of FAR 23.141 through 23.253 with any contamination on the aerodynamic surfaces normally encountered in service and to require that information relating to any resulting performance degradations be provided to the pilot....

Accordingly, the Federal Aviation Administration proposes the following special conditions as a part of the type certification basis for the Beech model 2000 series airplanes:....

4. Effects of Contamination on Laminar Flow Airfoils

In the absence of specific requirements for airfoil contamination, airplane airfoil designs that have airfoil pressure gradient characteristics and smooth aerodynamic surfaces that may be capable of supporting natural laminar flow must comply with the following:

- (a) It must be shown by tests or analysis supported by tests that the airplane complies with the requirements of FAR 23.141 through 23.253 with any airfoil contamination that would normally be encountered in service and which would cause significant adverse effects on the handling qualities of the airplane resulting from the loss of laminar flow.
- (b) Significant performance degradations identified as resulting from the loss of laminar flow must be provided as part of the information required by FAR 23.1585 and 23.1587.
...."

Similar conditions would be considered as part of the certification of any airplane with airfoil designs that have pressure gradient characteristics and smooth aerodynamic surfaces, which may be capable of supporting natural laminar flow.

Acknowledgements

The Dragonfly flight experiments, which provided some of the data for this paper, were conducted by Mr. Donald E. Hewes and the second author. These contributions by Mr. Hewes, who passed away in August 1985, are gratefully acknowledged.

References

- ¹Boeing Commercial Airplane Company, "F-111 Natural Laminar Flow Glove Flight Test Data Analysis and Boundary-Layer Stability Analysis," NASA CR-166051, Jan. 1984.
- ²Holmes, B. J., Obara, C. J., and Yip, L. P., "Natural Laminar Flow Experiments on Modern Airplane Surfaces," NASA TP-2256, June 1984.
- ³Croom, C. C. and Holmes, B. J., "Flight Evaluation of an Insect Contamination Protection System for Laminar Flow Wings," SAE Paper 850860, April 1985.
- ⁴Hall, G., "On the Mechanics of Transition Produced by Particles Passing Through an Initially Laminar Boundary Layer and the Estimated Effect on the LFC Performance of the X-21 Aircraft," Northrop Corp., Oct. 1964.
- ⁵Obara, C. J. and Holmes, B. J., "Flight-Measured Laminar Boundary-Layer Transition Phenomena Including Stability Theory Analysis," NASA TP-2417, April 1985.
- ⁶Harthun, M. H., Blumer, C. B., and Miller, B. A., "Orbiter Windward Surface Entry Heating: Post-Orbital Flight Test Program Update," *Shuttle Performance: Lessons Learned*, NASA CP-2283, Part 2, March 1983, pp. 781-804.
- ⁷Bragg, M. B. and Gregorek, G. M., "An Experimental Study of a High Performance Canard Airfoil with Boundary-Layer Trip and Vortex Generators," *Journal of Aircraft*, Vol. 24, May 1987, pp. 305-309.
- ⁸Nonweiler, T., "A New Series of Low-Drag Aerofoils," Department of Aeronautics and Fluid Mechanics, Univ. of Glasgow, Scotland, UK. Rept. 6801, 1968.
- ⁹Kelling, F. H., "Experimental Investigation of a High-Lift Low-Drag Aerofoil," Department of Aeronautics and Fluid Mechanics, Univ. of Glasgow, Scotland, U.K. Rept. 6802, 1968.
- ¹⁰Kelling, F. H., "Experimental Investigation of a High-Lift Low-Drag Aerofoil," Aeronautical Research Council Current Papers 1187, Sept. 1968.
- ¹¹Eppler, R. and Somers, D., "A Computer Program for the Design and Analysis of Low-Speed Airfoils," NASA TM-80210, 1980.
- ¹²Whitcomb, R. T., "A Design Approach and Selected Wind Tunnel Results at High-Subsonic Speeds for Wing Tip Mounted Winglets," NASA TN D-8260, July 1976.
- ¹³van Dam, C. P., "Natural Laminar Flow Airfoil Design Considerations for Winglets on Low-Speed Airplanes," NASA CR-3853, Dec. 1984.
- ¹⁴Yip, L. P. and Coy, P. F., "Wind-Tunnel Investigation of a Full-Scale Canard-Configured General Aviation Aircraft," ICAS Paper 82-6.8.2, 1982.
- ¹⁵Wentz, W. H., Jr., "Effectiveness of Spoilers on the GA(w)-1 Airfoil with a High-Performance Fowler Flap," NASA CR-2538, May 1975.
- ¹⁶Roskam, J., *Airplane Flight Dynamics and Automatic Flight Controls*, Roskam Aviation Engineering Corp., 1979.
- ¹⁷Holmes, B. J., Gall, P. D., Croom, C. C., Manuel, G. S., and Kelliher, W. C., "A New Method for Laminar Boundary-Layer Transition Visualization in Flight—Color Changes in Liquid Crystal Coatings," NASA TM-87666, Jan. 1986.
- ¹⁸Federal Aviation Administration, "Special Conditions; Beech Model 2000 Series Airplanes," *Federal Register*, Vol. 51, April 1986, pp. 11933-11942.

*Recommended Reading from the AIAA
Progress in Astronautics and Aeronautics Series . . .*



Monitoring Earth's Ocean, Land and Atmosphere from Space: Sensors, Systems, and Applications

Abraham Schnapf, editor

This comprehensive survey presents previously unpublished material on past, present, and future remote-sensing projects throughout the world. Chapters examine technical and other aspects of seminal satellite projects, such as Tiros/NOAA, NIMBUS, DMS, LANDSAT, Seasat, TOPEX, and GEOSAT, and remote-sensing programs from other countries. The book offers analysis of future NOAA requirements, spaceborne active laser sensors, and multidisciplinary Earth observation from space platforms.

TO ORDER: Write AIAA Order Department,
370 L'Enfant Promenade, S.W., Washington, DC 20024
Please include postage and handling fee of \$4.50 with all
orders. California and D.C. residents must add 6% sales
tax. All foreign orders must be prepaid.

1985 830 pp., illus. Hardback
ISBN 0-915928-98-1
AIAA Members \$59.95
Nonmembers \$99.95
Order Number V-97